

Low-temperature, low-frequency dielectric response of the pinned charge-density wave in $K_{0.3}MoO_3$

Jie Yang* and N. P. Ong

Joseph Henry Laboratories of Physics, Princeton University, Princeton, New Jersey 08544

(Received 1 March 1991)

The dielectric response of $K_{0.3}MoO_3$ is investigated at low temperatures ($10 < T < 40$ K) and low frequencies ($1 < \omega < 10$ kHz). We observe a low-frequency mode that remains well defined at a frequency of 1 Hz (at 33 K). The peak value of the dielectric function $\epsilon_1(\omega)$ associated with this mode grows monotonically as T decreases. We compare our measurements with a recent model of Littlewood that identifies the low-frequency mode with the longitudinal response of the pinned charge-density wave.

I. INTRODUCTION

The dielectric response of the pinned charge-density wave (CDW) has been the subject of several studies.¹⁻⁸ In the pinned state, the “resonance” frequency of the CDW lies in the microwave region.⁸ The behavior of the dielectric response may be divided into a high-frequency and a low-frequency regime. At microwave frequencies (higher than 1 GHz), the spectrum appears to be well described by an over-damped Lorentzian oscillator. Extensive measurements up to the 100-GHz range have been reported by Reagor *et al.*^{6,7} on TaS_3 , $(TaSe_4)_2I$, and $NbSe_3$. In the low-frequency regime (less than 10 MHz), the response in the semiconducting compounds [$K_{0.3}MoO_3$, TaS_3 , and $(TaSe_4)_2I$] is strongly dispersive and temperature dependent. In $K_{0.3}MoO_3$ (“blue bronze”) the dielectric spectrum between 5 Hz and 13 MHz was studied by Cava *et al.*¹ at temperatures down to 40 K. Measurements in TaS_3 over a similar range have also been reported by several groups.²⁻⁵

In these studies, the low-frequency dielectric function $\epsilon(\omega) = \epsilon_1 + i\epsilon_2$ is usually fitted^{1,3-5} to (extensions of) the Cole-Davidson expression, which imply the existence of a very broad distribution of time scales. With decreasing temperature, the fits show that the time scales rapidly shift to low frequencies. Recent progress in analyzing the low-frequency behavior derives from studying the relaxation of the CDW, via its coupling to free carriers.^{9,10} Littlewood¹⁰ has shown that, when the pinning potential is disordered, a fraction (predominantly longitudinal) of the oscillator strength in the pinned mode splits off and decreases to low frequencies as the free-carrier density decreases. This low-frequency mode dominates the dielectric response at low temperatures. Extension of the dielectric studies to temperatures below 40 K, with the new perspective in mind, seems highly desirable. A second motivation is the interesting question of the behavior of $\epsilon_1(\omega)$ in the limit of zero frequency. In their study on blue bronze, Cava *et al.*¹ report that $\epsilon_1(\omega)$ (above 40 K) saturates to a large but finite value in the limit $\omega \rightarrow 0$, whereas ϵ_2 decreases to zero. However, Wu *et al.*² find that, in the compound TaS_3 , ϵ_1 measured at 120 K goes as $\omega^{-0.1}$ for frequencies down to 10 Hz, sug-

gesting a divergent polarizability. In subsequent studies, other groups³⁻⁵ have not observed the divergence, and this remains an unsettled issue.

To address these issues, we have measured the dielectric response of $K_{0.3}MoO_3$ at frequencies between 1 Hz and 10 kHz over the temperature range 10–70 K. At temperatures that overlap the study of Cava *et al.*¹ (above 40 K), we find quite good agreement with their measurements. Below 40 K, we uncover a broad low-frequency mode that remains well defined down to 1 Hz (as the temperature decreases). By extrapolation, we relate the center frequency of this mode ω_s to the time scale τ_0 previously obtained by Cava *et al.* In our data, the mode behavior is much better defined, so that it can be tracked to lower temperatures. Our results show that, below 25 K, $\epsilon_1(\omega)$ increases to very large values as both ω and T decrease towards zero. However, the rapid increase of the time scale $1/\omega_s$ to exponentially large values precludes a definitive determination of the value of $\epsilon_1(\omega)$ in the true zero-frequency limit.

II. EXPERIMENTAL DETAILS

Samples are cleaved from a large crystal and cut into millimeter-sized rectangular bars. Using silver paint, we attach gold wires (50 μm) to indium films (2000 Å thick) evaporated onto the end faces of the crystal. The applied ac current flows parallel to the most highly conducting axis. The sample is thermally anchored to a sapphire substrate bonded to a large gold-plated copper block which houses the Ge thermometer used for temperature sensing. The copper block is sealed in a vacuum can which is suspended above liquid helium. The ac voltage from a sine wave source is stepped down using a ratio transformer (Gertsh VRT-7R), and then applied to the sample, which is connected in series with a 1 M Ω reference resistor R_0 . The sample voltage V_s is detected by a dual-channel lock-in amplifier (PAR 5204). V_s is given by $V_s/V_0 = (1 + R_0 Y)^{-1}$, where V_0 (≈ 1 mV) is the output of the transformer, and $Y = Y_1 + iY_2$ the sample admittance. We made sure that our measurements were in the linear regime by varying the current over a decade. The sample voltage V_s is measured at fixed ω with the

temperature slowly drifting at a rate of 1 K/min. Data are taken by a computer for both warming and cooling directions. No thermal hysteresis was detected below 50 K. Three samples were measured, with similar results.

The large impedance encountered below approximately 30 K requires some careful experimental attention. If the admittance of the sample is expressed as a capacitance, the real part C_1 (imaginary part C_2) varies from 200 pF (200 pF) at 10 K to 20 nF (400 nF) at 60 K at an excitation frequency of 1 kHz. The loss tangent factor C_2/C_1 is large (typically approximately 20 at 60 K) and strongly dependent on T and ω above 20 K. Below 20 K, however, it decreases rapidly to a temperature-independent value near 1. Below 30 K (when $R_0|Y| \ll 1$), the measurements are especially sensitive to errors in the phase setting. In this limit, the real and imaginary parts of V_s become

$$\text{Re}V_s \approx V_0(1 - R_0Y_1), \quad \text{Im}V_s \approx -V_0R_0Y_2. \quad (1)$$

It is clear from Eq. (1) that errors in the phase setting strongly distort the inferred value of Y_2 , which is our main quantity of interest. To get estimates of errors, we repeated some runs with intentionally introduced phase offsets varying from 0.4° to 5° (of either sign). (To eliminate errors from line-impedance contributions, we carefully nulled the phase by replacing the sample with either a 1 or 10 k Ω metal-film resistor before the start of each experiment. The phase stability of the lock-in amplifier is estimated to be $\pm 0.1^\circ$ near 3 Hz.) We find that offsets in the phase as small as 0.4° are sufficient to change the inferred Y_2 by a factor of 10. Adopting a conservative margin of safety, we disregard results in frequency and temperature regimes in which $\text{Im}V_s$ is less than 1% of $\text{Re}V_s$ (i.e., $Y_2 < 10^{-8}$ S). This restricts the data to what is reproduced in Figs. 1 and 2. (For example, at tempera-

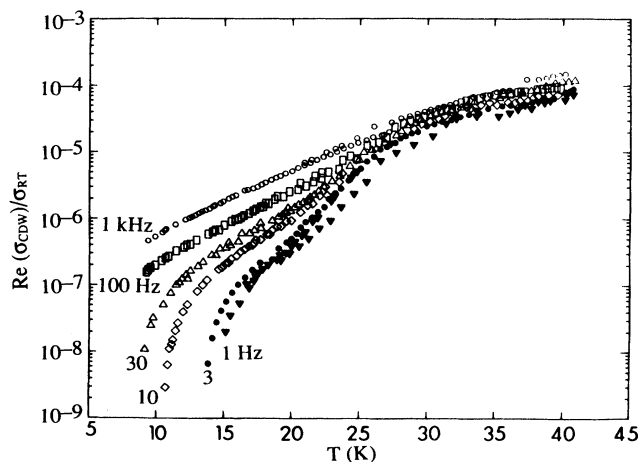


FIG. 1. Temperature dependence of the real part of the CDW conductivity normalized to the conductivity at room temperature at frequencies between 1 Hz and 1 kHz in $\text{K}_{0.3}\text{MoO}_3$ (sample 1, size $0.6 \times 2.0 \times 2.3$ mm 3). At each frequency, σ_{CDW} is obtained by subtracting σ_0 from the total ac conductivity.

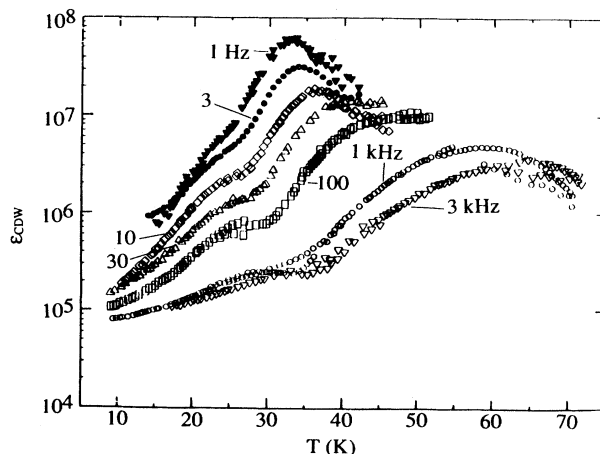


FIG. 2. Temperature dependence of the real part of the dielectric response $\epsilon_1(\omega) = \epsilon_{\text{CDW}}$ of the pinned CDW in $\text{K}_{0.3}\text{MoO}_3$ (sample 1). At each frequency, the peak in $\epsilon_1(\omega)$ vs T defines the frequency scale ω_s [Eq. (2)].

tures above 45 K, the data for C_1 at 3 Hz are rejected because the phase resolution required exceeds our confidence level.)

III. EXPERIMENTAL RESULTS

Over our range of temperature, the dc conductivity due to the free carriers σ_0 follows an activated behavior with an activation gap Δ_{dc} of 700 K. The ac conductivity σ_{CDW} of the pinned CDW is obtained by subtracting σ_0 from the total ac conductivity $\omega\epsilon_2\epsilon_0$ (ϵ_0 is the permittivity). The temperature dependence of σ_{CDW} (normalized to the value of σ_0 at room temperature) is displayed in Fig. 1 at selected frequencies between 1 Hz and 1 kHz. Dispersion in σ_{CDW} becomes increasingly pronounced below 20 K even at our lowest frequency 1 Hz.

The low-temperature dispersion is more apparent when we plot the temperature dependence of the dielectric constant $\epsilon_1(\omega) = \epsilon_{\text{CDW}}(\omega)$ of the pinned CDW (Fig. 2). At our lowest temperature, 10 K, $\epsilon_1(\omega)$ is very large, decreasing from 2×10^5 at 10 Hz to 8×10^4 at 3 kHz. With increasing temperature, $\epsilon_1(\omega)$ rises to a fairly sharp maximum at a temperature that depends sensitively on ω . In previous measurements, which terminate at 40 K, the maximum in $\epsilon_1(\omega)$ is discernible, but very broad, so that little attention has been paid to it in the literature (open symbols in Fig. 3).

Our main finding in this report is that the peak becomes increasingly well defined as we move to lower frequencies and temperatures. The magnitude of $\epsilon_1(\omega)$ at the peak is finite, although anomalously large (6×10^7 at 1 Hz in sample 1). The large values reflect the extreme polarizability of the pinned CDW. The results in Fig. 2 show that, at low temperatures, the peak in $\epsilon_1(\omega)$ becomes the most prominent feature of the frequency response at low frequencies. As the temperature de-

creases below the peak value, $\epsilon_1(\omega)$ plummets rapidly. [At 1 Hz, $\epsilon_1(\omega)$ decreases by two orders of magnitude in a 20-K interval.] It is natural to identify the frequency scale of the low-frequency mode (ω_s) with the peak in $\epsilon_1(\omega)$ in Fig. 2, i.e., the peak position provides the temperature dependence of ω_s . From our data below 100 Hz, we find that ω_s has the activated form

$$\omega_s = \omega_{s0} \exp(-\Delta/T), \quad (2)$$

with $\omega_{s0}/2\pi = 2.95 \times 10^9 \text{ s}^{-1}$ and $\Delta = 708 \text{ K}$. [The value of Δ agrees well with Δ_{dc} ($\sim 700 \text{ K}$) obtained from σ_0 . The time scale $1/\omega_s$ is quite close to the characteristic time τ_0 that Cava *et al.*¹ extract from a fit of their spectra to a generalization of the Cole-Davidson type of dispersion for the dielectric function. τ_0 is also activated, with a gap value (829 K) slightly larger than in Eq. (2).] The prominence of the peak in ϵ_1 implies that the linear response of $\text{K}_{0.3}\text{MoO}_3$ at cryogenic temperatures to abrupt changes in applied field (pulses) is largely dictated by the time scale $1/\omega_s$ (or τ_0).

It is also useful to convert the dielectric response data

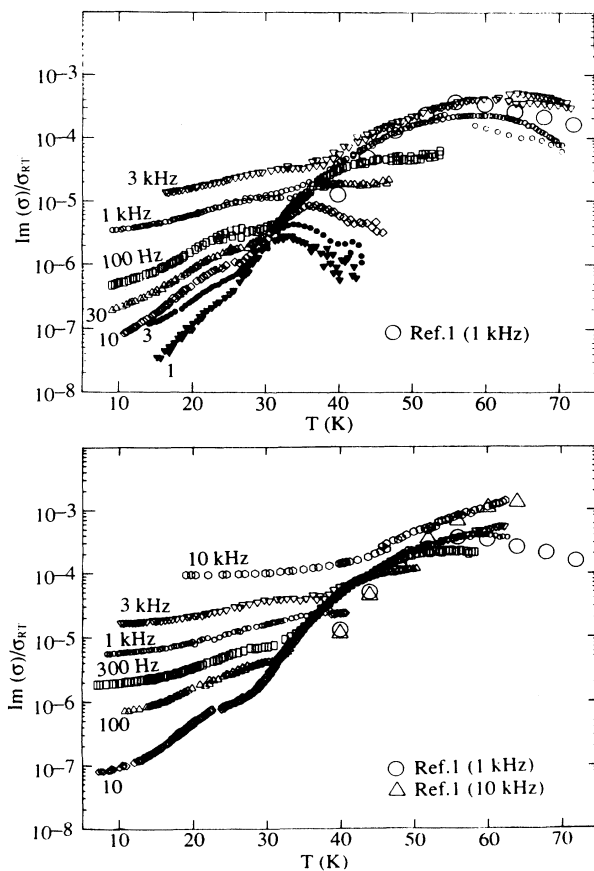


FIG. 3. The same data in Fig. 2 replotted as the imaginary part of the ac conductivity ($\text{Im}\sigma = \omega\epsilon_1$) normalized to σ_0 at room temperature. The upper (lower) panel show data for sample 1 (2). The size of sample 2 is $0.3 \times 0.9 \times 1.4 \text{ mm}^3$.

to the ac conductivity of the pinned CDW via $\text{Im}\sigma_{\text{CDW}} = \omega\epsilon_1(\omega)\epsilon_0$. In Fig. 3 we show $\text{Im}\sigma_{\text{CDW}}$ normalized to σ_0 at room temperature for samples 1 (upper panel) and 2 (lower). For comparison, we also show results from Cava *et al.*¹ (open symbols) where our measurements overlap with his.

IV. DISCUSSION

To examine the frequency dependence of the dielectric response, we replot in Fig. 4 $\text{Im}\sigma_{\text{CDW}}$ versus frequency at temperatures 15–40 K. (Figure 4 extends the data in Fig. 2 of Cava *et al.*,¹ which covers the temperature range from 40 to 110 K.) The 40-K curve in our sample agrees well with that of Cava *et al.*, apart from a vertical scale factor. As the frequency decreases from 3 kHz, $\text{Im}\sigma_{\text{CDW}}$ goes through a broad maximum (the analog of the peak in Fig. 2 in the frequency domain). At frequencies below the maximum, $\text{Im}\sigma_{\text{CDW}}$ decreases as ω^n where $n = 1.0 \pm 0.1$. (This exponent is more reliably obtained from the data of Cava *et al.*, which extend to higher temperatures.) Thus the dispersion of $\text{Im}\sigma_{\text{CDW}}$ is linear in ω for $\omega < \omega_s$, implying that $\epsilon_1(\omega)$ approaches a constant value as $\omega \rightarrow 0$, i.e., the limit

$$\lim_{\omega \rightarrow 0} \epsilon_1(\omega, T) = \epsilon(0, T) \quad (3)$$

is finite for $T \geq 40 \text{ K}$.

It is now interesting to examine the evolution of the spectrum as the temperature falls below 40 K. With decreasing T , the broad maximum moves to lower frequency. As evident in the 30-K curve, the downward shift of the broad mode uncovers a “background” dispersion which also follows a power law. (In a plot versus the fre-

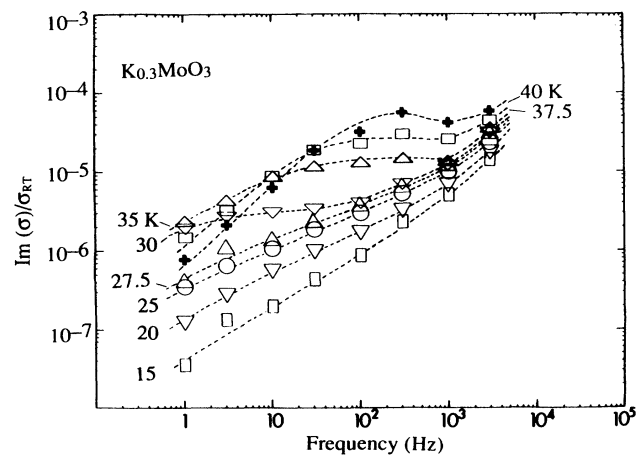


FIG. 4. The frequency dependence of $\text{Im}\sigma \approx \omega\epsilon_1$ at temperatures 15–40 K. The broad maximum clearly discernible in the 40-K curve exponentially shifts to lower frequencies with decreasing temperature. The slope of the 15-K curve corresponds to a power-law dependence $\text{Im}\sigma \approx \omega^{0.28}$. This figure extends Fig. 2 of Cava *et al.* (Ref. 1) to lower temperatures.

quency, the broad mode is approximately centered at the frequency ω_s .) Below 20 K, most of the broad mode has decreased below 1 Hz. What remains in the 15-K curve is a power-law dispersion ω^α that we identify with the intermediate frequency regime. From the 15-K data, we estimate α to be 0.72 ± 0.05 .

As mentioned in the Introduction, the remarkable migration of the ω_s mode to ultralow frequencies with decreasing temperature complicates the question of whether $\epsilon(0, T)$ introduced in Eq (3) exists in the limit $T \rightarrow 0$. In practical terms, this means that one cannot answer experimentally the question posed by Eq. (3) for temperatures lower than ≈ 25 K. At these temperatures, $\epsilon_1(\omega)$ appears to diverge as $\omega^{-(1-\alpha)} \approx \omega^{-0.3}$, for frequencies above 1 Hz. However, since ω_s is smaller (by several orders of magnitude) than 1 Hz, this represents the behavior in the *intermediate* frequency range. [Equation (2), if it persists, implies that $1/\omega_s$ rapidly grows to experimentally inaccessible values (approximately 9 days at 20 K; 3400 y at 15 K).] In order to access the true low-frequency regime of $\epsilon_1(\omega)$, it is necessary to go to time scales longer than $1/\omega_s$. Thus it is all but impossible to reach the “true” zero-frequency limit of $\epsilon_1(\omega)$ at these low temperatures. The solution to the question of the divergence of ϵ_{CDW} at low frequencies depends critically on the temperature. The limit $\epsilon(0, T)$ is finite for temperatures above approximately 25 K; below 25 K, however, the answer depends on whether we are willing to entertain extremely long experimental time scales and to exclude the intrusion of other scales.

The activated behavior in Eq. (2) and the similar values for Δ and Δ_{dc} suggest that the thermally activated free carriers play a central role in defining the peak in ϵ_1 . We recall that, in the regime where the CDW is depinned by an applied electric field, there exists strong evidence that the free carriers provide the primary damping for CDW motion. In both the metallic¹¹ (NbSe₃) and semiconducting compounds¹² (K_{0.3}MoO₃, TaS₃) the CDW nonlinear current (in high electric fields) scales with the Ohmic conductivity σ_0 ; this indicates that the moving CDW interacts strongly with the free carriers. The coupling presumably remains strong in the pinned state. Thus it is natural to interpret Eq. (2) as evidence for strong coupling of the pinned CDW to the thermally generated free carriers.

In Littlewood’s model,¹⁰ the longitudinal mode (which couples to the electrostatic potential) is distinguished from the transverse mode, which couples to electromagnetic radiation. When disorder in the pinning potential is large, a uniform ac current with zero wave vector \mathbf{q} excites finite- \mathbf{q} modes, which represent inhomogeneous distortions of the condensate. The flow of free electrons which attempt to screen the inhomogeneous charge distribution leads to damping of the CDW. As a result of the coupling, the longitudinal mode splits off from the main mode, and moves to lower ω . A peak in ϵ_2 (or a shoulder in ϵ_1) appears at the frequency $1/\tau_1$, which has an activated behavior, with energy equal to the single-

particle gap. Our results are qualitatively consistent with this scenario, if we identify ω_s (or $1/\tau_0$) with $1/\tau_1$. However, in the model,¹⁰ the peak value of ϵ_1 at zero ω is independent of $1/\tau_1$ (i.e., temperature), in contrast to our results which show that the peak value increases monotonically as ω_s decreases (Fig. 2). This seems to indicate that an essential ingredient is missing in the characterization of the longitudinal mode. The monotonic increase of ϵ_1 at the peak, in fact, suggests a divergence of the polarizability as T approaches 0. (However, as we argue above, the true zero-frequency limit cannot be reached at low temperatures, so that this point is very difficult to confirm experimentally.) Related experiments are the observed divergence of the dielectric polarization near the threshold for the onset of sliding motion. Pulsed experiments have been reported by Wang and Ong¹³ and by Chen, Mihály, and Grüner.¹⁴

V. SUMMARY

The present measurements of the dielectric function of the pinned CDW extend to temperatures lower than previously reported. We uncover a low-frequency mode centered at the frequency ω_s , which rapidly moves to ultralow frequencies as the temperature decreases below 40 K. Although this mode is discernible in previous results, we show that it becomes especially well defined in a plot of ϵ_1 versus temperature at fixed ω (Fig. 2). The activated behavior of ω_s is consistent with the notion that relaxation of the deformed CDW is controlled by the density of free carriers, which screen the strong Coulomb forces arising from inhomogeneous deformations of the CDW.^{9,10} The existence of the activated low-frequency mode complicates the question whether ϵ_1 has a meaningful zero-frequency limit at low temperatures. The frequency spectrum (Fig. 4) shows that ϵ_1 changes from a fractional power-law behavior $\omega^{-0.3}$ above ω_s to a frequency-independent behavior $\sim \omega^0$ below ω_s . Thus, for any finite frequency window, the rapid migration of the ω_s mode across this window, with decreasing temperature, converts the spectrum from the low-frequency regime to the less-interesting intermediate regime. At low temperatures, the time scale $1/\omega_s$ grows to exponentially large values, rendering the former regime experimentally inaccessible. At temperatures higher than approximately 30 K, however, measurements in the low-frequency regime ($\omega < \omega_2$) are feasible. $\epsilon_1(0)$ may be shown to have an experimentally well-defined value, which is very large, but nonetheless finite.

ACKNOWLEDGMENTS

We wish to thank Professor George Grüner for providing the samples. Partial support from the Seaver Institute is gratefully acknowledged.

*Present address: Department of Physiology, Jordan Hall, Box 449, University of Virginia, Charlottesville, VA 22908.

- ¹R. J. Cava, R. M. Fleming, P. Littlewood, E. A. Rietman, L. F. Schneemeyer, and R. G. Dunn, *Phys. Rev. B* **30**, 3228 (1984).
- ²W. Y. Wu, L. Mihály, G. Mozurkewich, and G. Grüner, *Phys. Rev. Lett.* **52**, 2382 (1984).
- ³J. P. Stokes, M. O. Robbins, and S. Bhattacharya, *Phys. Rev. B* **32**, 6939 (1985).
- ⁴R. J. Cava, R. M. Fleming, R. G. Dunn, and E. A. Rietman, *Phys. Rev. B* **32**, 8325 (1985).
- ⁵R. J. Cava, P. Littlewood, R. M. Fleming, R. G. Dunn, and E. A. Rietman, *Phys. Rev. B* **33**, 2439 (1986).
- ⁶D. Reagor, S. Sridhar, and G. Grüner, *Phys. Rev. B* **34**, 2212 (1986).
- ⁷D. Reagor, S. Sridhar, M. Maki, and G. Grüner, *Phys. Rev. B* **32**, 8445 (1985).
- ⁸N. P. Ong and P. Monceau, *Phys. Rev. B* **16**, 3443 (1977).
- ⁹W. L. McMillan, *Phys. Rev. B* **12**, 1197 (1975); R. N. Bhatt and W. L. McMillan, *ibid.* **12**, 2042 (1975); L. Sneddon, *ibid.* **29**, 719 (1984).
- ¹⁰P. B. Littlewood, *Phys. Rev. B* **36**, 3108 (1987).
- ¹¹X. J. Zhang and N. P. Ong, *Phys. Rev. Lett.* **55**, 2919 (1985).
- ¹²R. M. Fleming, R. J. Cava, F. Schneemeyer, E. A. Rietman, and R. G. Dunn, *Phys. Rev. B* **33**, 5450 (1986).
- ¹³Z. Z. Wang and N. P. Ong, *Phys. Rev. Lett.* **58**, 2375 (1987).
- ¹⁴T. Chen, L. Mihály, and G. Grüner, *Phys. Rev. Lett.* **60**, 464 (1988).